ANALYSIS OF VEHICLE BODY WITH SMALL-OVERLAP FRONTAL IMPACT ON VARIOUS BARRIERS

Phd. Luu Nguyen Phu Thuong*, Duy Quoc Tran
Ly Tu Trong Technical College of Ho Chi Minh

ABSTRACT–This paper presents an analysis of the vehicle structure in the event of a small-overlap frontal impact (SOFI) on various barriers based on a computer crash simulation model. Three barrier models were developed for SOFI simulation based on real test conditions: Flat 50, Flat 150, and Pole 250. The simulation models were developed using HyperMesh and LS-DYNA software. The crash simulation results were used to evaluate the overall vehicle structure through a comparison of intrusion measurements with the rating guidelines of the Insurance Institute for Highway Safety. The parts sensitive to a small-overlap crash were confirmed. Thickness optimization was conducted to strengthen the rocker panel, A-pillar, and lower hinge pillar in order to improve the vehicle structure in the event of a SOFI. The best values among the variables were chosen for the new design. The crash analysis using finite element models showed that the most serious damage to the vehicle structure occurred when the minivan model collided with Flat 50 at 20% overlap. In this study, the grade of the overall structure was changed from "poor" to "acceptable" in the case of Pole 250.

KEY WORDS: small-overlap, crashworthiness, frontal impact, vehicle structure, barrier design, crash test.

1. INTRODUCTION

The Insurance Institute for Highway Safety (IIHS) introduced the small-overlap frontal impact (SOFI) test in 2012 in order to consider one of the most serious crash scenarios and difficult engineering challenges [1-3]. During the experiment, the vehicle hits a rigid wall at 64 km/h with 25% of the front bumper making contact with the barrier. A real-life comparison may be a vehicle colliding with a pole or flat object but only making contact with the center-line of the headlight [4].

In small-overlap frontal crashes, the crash forces are applied outboard of the vehicle's longitudinal frame rails [5]. In addition, forces are concentrated on the front suspension, at the firewall, and at the base of the A-pillar. These areas not traditionally designed to absorb and dissipate crash forces [6 - 8].

In recent studies on small-overlaps, two vehicles have been developed with different types of rail cross-sections along the longitudinal direction. Finite element (FE) analysis was performed to characterize the frontal pole impact compared to the full-frontal rigid barrier test and IIHS 40% offset frontal impact test. Hong et al. found that the rails absorbed over 50% of the crash energy in the IIHS test [9]. Park et al. suggested that the offset-frontal crash test can be used to complement the full-frontal crash test [10].

Chen et al. investigated vehicle-side impacts and showed that mass could be conserved without compromising the side impact crash test performance by using advanced high strength steels and optimized cross-sections of the structural components [11].

Recently, researchers have studied vehicle structures to improve the frontal crashworthiness. Halloway et al. proposed classifiers to indicate the number of longitudinal members [12]. Jakobsson et al. described the significance and developments of two decades of car design for applications to severe frontal collisions with partial overlap [13]. The minimization of weight and competing requirements from several load cases have to be adjusted to be as optimal as possible. Chittepu analyzed an insurance crash load case to demonstrate several additional benefits of robustness analysis for virtual product development [14]. However, most of these studies only considered one berrier case.

For the current research topic, there have been no published works so far. New barrier designs are updated on the IIHS small-overlap research program [1, 15]. Which are used in SOFI experiments. The purpose of this study was to compare overall structural ratings of vehicles in the event of a SOFI on the basis of different barrier crash test simulations. A size optimization method is proposed to improve a vehicle's structural resistance to a SOFI. The thicknesses of the A-pillar, rocker panel, and hinge pillar were changed to reinforce the car body. The optimization designs with the best crashworthiness intrusion results were chosen for comparison with the original model. In this study, a minivan computer model [16] was applied to a real IIHS crash test [2] using LS-DYNA [17] software for the crash test simulations.

Following the introduction, section 2 reviews the current standard crash tests. Section 3 presents the FE model used for verification and validation. Barrier models

* *Corresponding author*. e-mail: luunguyenphuthuong@gmail.com

were developed for SOFIs. Section 4 presents the model experiment to characterize the SOFI test simulation. The simulation results were applied to rate the full vehicle structure and to optimize the design of the car body. Finally, this paper concludes with a discussion of possible future extensions of this research.

2. CURRENT STANDARDS CRASH TEST

The Federal Motor Vehicle Safety Standard (FMVSS) was developed and enforced by the National Highway Traffic Safety Administration (NHTSA) in 1966. The FMVSS 208 sets performance requirements for occupant protection in the event of a frontal crash, these are measured by using anthropomorphic test devices (dummies) located in the front seats. Typically, the test involves launching a full-scale vehicle to impact a rigid barrier at 48 km/h at 90^o to the barrier surface [6].

The New Car Assessment Performance (NCAP) test was initiated by NHTSA in the early 1980s. It is identical to FMVSS 208 except that the impact speed is 56 km/h and the front dummies are restrained by lap/shoulder belts in addition to the passive air-bag [6].

Modern cars often perform poorly in the IIHS' new small-overlap crash test. This frontal impact test demonstrates what happens when only a small part of the front of the vehicle collides with another vehicle or an object such as a pillar or tree. Whereas the Euro-NCAP crash test is carried out at 64 km/h and 40% overlap with a deformable barrier, the IIHS test uses the same velocity but 25% overlap with a rigid flat barrier [18]. In 2013, the IIHS reduced the overlap to only 20% [1, 15].

3. SMALL-OVERLAP MODELING

3.1. Description and validation of vehicle FE model

A minivan FE model [16] was used in this study for experiments based on updates to the IIHS small-overlap research program [1, 15]. The FE model from the National Crash Analysis Center library [21] contains of 333,455 elements without interior components or restraint systems. The detailed FE model was constructed of parts broken down into elements.

The set of elements representing the vehicle was translated into an FE model, each element was defined as a shell, beam, or solid element in accordance with the requirements for using LS-DYNA software [17].

The developed FE model [16] had the following characteristics:

Number of parts:	- 510
Number of nodes:	- 344,724
Number of shells:	- 327,163
Number of beams:	- 35
Number of solids:	- 6,253

The FE model was verified and validated in several ways to ensure that it was an accurate representation of the actual vehicle. These efforts included checking for the completeness of elements and adequacy of the connection details. This model was validated by comparing the test and simulation results for the acceleration and energy absorption of the vehicle according to [21].

Figure 1 plots the global energy from the simulation. The energy was balanced throughout the simulation. The simulation started with an initial amount of kinetic energy, and no external work was applied. As the simulation progressed, the kinetic energy decreased, and the internal energy increased because of the impact with the wall. The total energy remained constant in the simulation since no external work was applied to the vehicle.

The curve shapes and peak value of the model showed good and consistent correlation with [16]. The agreement with regard to the acceleration (Figure 2), energy curve (Figure 1) and velocity (Figure 3) meant that this FE model could be assumed to be valid.

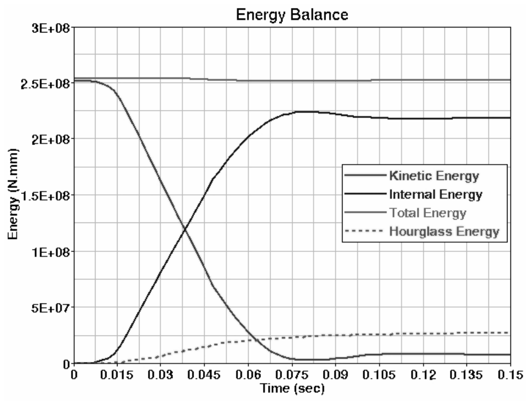

Figure 1. Simulation energy balance analyses

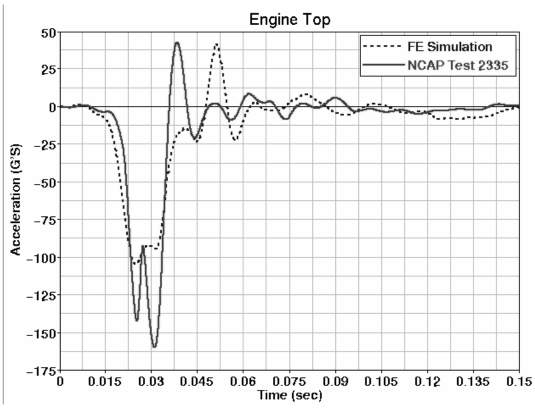

Figure 2. Test and simulation results for engine top acceleration vs time curve

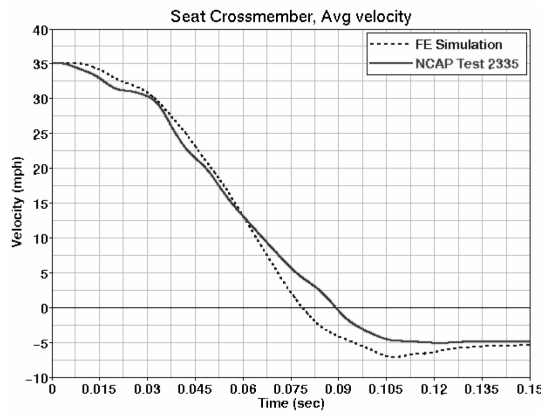

Figure 3. Test and simulation results for seat cross member average velocity curve

3.2. Barrier model designs

In this study, three barrier types were designed, as shown in Figure 4: Flat 150 was a flat barrier with a 150 mm radius and 25% overlap [1], Flat 50 was a flat barrier with a 50 mm radius and 20% overlap [2]; and Pole 250 was a pole with a 250 mm radius and 25% overlap [2].

The two proportions to the vehicle width modes were 20% and 5%, as shown in Figure 5. Most of the barriers for the experiments were made using the CATIA software. HyperMesh was then used to derive their FE models. As shown in Figure 6, these two modes were used to develop three FE simulation models.

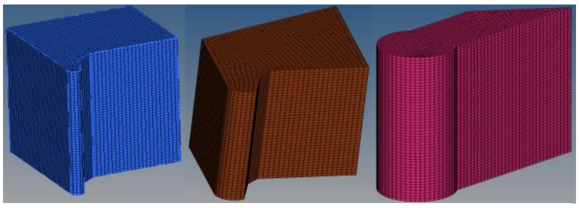

Figure 4. (a) Flat 50 (b) Flat 150 (c) Pole 250

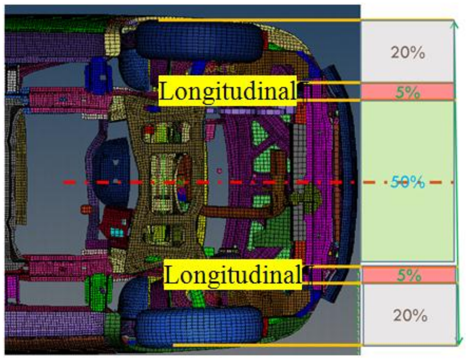

Figure 5. Vehicle width ratio and structure of minivan model

3.3. Small-overlap crash test model

The small-overlap crash examination model was set to follow the actual IIHS crash test conditions. The right edge of the barrier model face was offset to the left of the vehicle centerline by 20% or 25% depending on the type of barrier and the minivan model hit it at 64 km/h.

Figure 7 shown the measurement points to mearsure vehicle intrusion. Following [2], 18 points were measured. The scope of this study was improving the frontal structure in the event of a SOFI, so only nine points were used to measure deformation: the lower (three points) and upper (three points) hinge pillar, and the rocker panel (three points). The hinge pillar was measured at the inner-most surface of the door opening; this was typically on the pinch weld.

The vertical coordinates for the three lower points were obtained by adding 0 cm (lower hinge pillar point 1), 7.5 cm (lower hinge pillar point 2), and 15 cm (lower hinge pillar point 3) to the brake pedal reference point. The upper points were obtained by adding 45 cm (upper hinge pillar point 1), 52.5 cm (upper hinge pillar point 2), and 60 cm (upper hinge pillar point 3).

The rocker panel was also measured at the inner-most surface of the door opening; this was typically on the pinch weld. The longitudinal coordinates were obtained by adding 20 cm (rocker panel point 1), 35 cm (rocker panel point 2), and 50 cm (rocker panel point 3) to the brake pedal reference point.

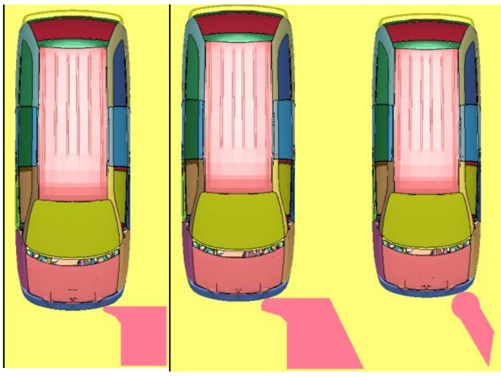

(a)Flat 50 (b) Flat 150 (c) Pole 250

Figure 6. FE simulations models for three barriers

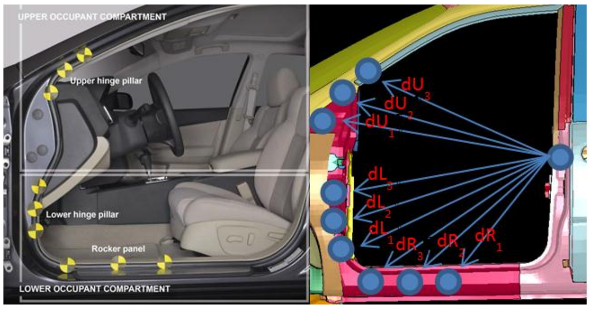

Figure 7. Measurement points in occupant compartment

The formulation to calculate the intrusion dimensions in Table 1 are presented below in Equations (1)-(12).

Table 1. Component dimensions pre- and post-crash

Components	Pre-crash	Post-crash	Intrusion
Rocker panel 1	dR1	d'R1	R1
Rocker panel 2	dR2	d'R2	R2
Rocker panel 3	dR3	d'R3	R3
Lower hinge pillar 1	dL1	d'L1	L1
Lower hinge pillar 2	dL2	d'L2	L2
Lower hinge pillar 3	dL3	d'L3	L3
Upper hinge pillar 1	dU1	d'U1	U1
Upper hinge pillar 2	dU2	d'U2	U2
Upper hinge pillar 3	dU3	d'U3	U3
Rocker panel			**R**
Lower hinge pillar			**L**
Upper hinge pillar			**U**

$$R_1 = dR_1 - d'R_1 \quad (1)$$
$$R_2 = dR_2 - d'R_2 \quad (2)$$
$$R_3 = dR_3 - d'R_3 \quad (3)$$
$$L_1 = dL_1 - d'L_1 \quad (4)$$
$$L_2 = dL_2 - d'L_2 \quad (5)$$
$$L_3 = dL_3 - d'L_3 \quad (6)$$
$$U_1 = dU_1 - d'U_1 \quad (7)$$
$$U_2 = dU_2 - d'U_2 \quad (8)$$
$$U_3 = dU_3 - d'U_3 \quad (9)$$
$$R = \frac{R_1 + R_2 + R_3}{3} \quad (10)$$
$$L = Max\,(L_1 : L_3) \quad (11)$$
$$U = Max\,(U_1 : U_3) \quad (12)$$

4. SMALL-OVERLAP TEST SIMULATIONS

4.1. Frontal crash simulation of full vehicle model

The contact area in a small-overlap crash is tiny compared with the full width of the car model; thus, the body is serious damaged during the impact. Figure 8 shows the resulting damage to the frontal structure of the vehicle models in the three impact modes.

The intrusion of the frontal compartments was selected as the parameter for measuring the damage severity. Table 2 presents the intrusion values in the three collision modes.

Figure 9 compares the three modes; Table 2 lists the values. The detailed analysis of the simulation results is presented below.

With Flat 50, the left longitudinal rail was largely undamaged. This means that the majority of the loading was outside longitudinal structures such as the rocker arm and hinge pillar. Figure 10 shows that the upper hinge pillar was the most deformed part in this case. The red dotted line in Figure 13 shows that the main longitudinal rail was missed. The wheel was directly loaded and pushed rearward into the toepan. The hinge pillar, rocker panel, and upper structures experienced additional loading. This loading pattern led to significant intrusion of both the lower and upper regions of the occupant compartment, as shown in Figure 9. In this case, the wheel suffered from the load; this caused distortion and a rotation 90^o, which caused nearly the whole body of the vehicle to twist.

The second mode was Flat 150; the result was shown in Figure 11. In this case, the main longitudinal rail was not missed, so the left wheel was not directly loaded. This was why Flat 150 received less damage than Flat 50. The blue line in Figure 13 show the path load; the upper hinge pillar was the most deformed, as shown in Figure 9.

The last mode was Pole 250; the result was shown in Figure 12. In this case, the same situation as for Flat 150 occurred; this was shown by the gold line load path in Figure 13. The vehicle model tended to rotate and slide sideways during this type of collision; this can move the driver's head outboard away from the protection of the front airbag. In this mode, the vehicle model quickly moved out to the side; thus, it received less damage than in the other modes.

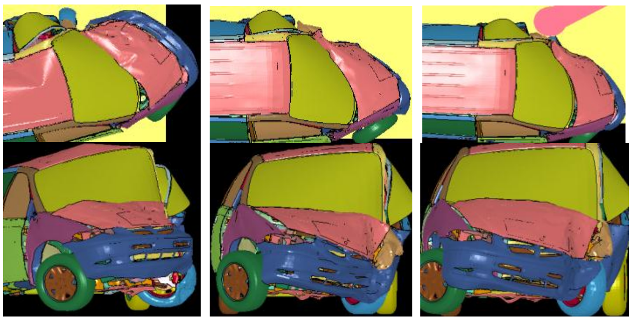

(a) Flat 50 (b) Flat 150 (c) Pole250

Figure 8. Top and back views for intrusion of three impact modes.

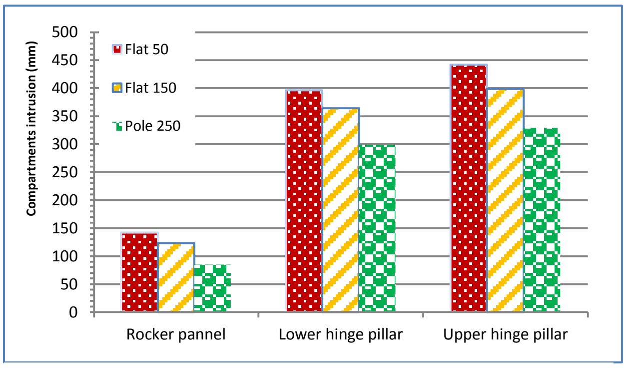

Figure 9. Comparison of occupant compartments in three modes

Table 2. Intrusion of occupant compartments in three modes (unit: mm)

Components	Pre-crash	Post-crash Flat 50	Intrusion	Post-crash Flat 150	Intrusion	Post-crash Pole 250	Intrusion	Note
Rocker pannel 1	838.419	753.071	85.348	736.532	101.887	760.166	78.253	
Rocker pannel 2	944.33	803.388	140.942	842.595	101.735	859.886	84.444	
Rocker pannel 3	1027.21	826.769	200.441	861.11	166.1	935.391	91.819	
Lower hinge pillar 1	1044.33	650.408	393.922	728.952	315.378	746.002	298.328	
Lower hinge pillar 2	1037.52	641.279	396.241	673.356	364.164	788.296	249.224	
Lower hinge pillar 3	1007.28	631.512	375.768	649.543	357.737	746.518	260.762	
Upper hinge pillar 1	1108.32	759.48	348.84	710.069	398.251	779.035	329.285	
Upper hinge pillar 2	1039.12	597.225	441.895	656.424	382.696	798.479	240.641	
Upper hinge pillar 3	967.053	658.669	308.384	693.952	273.101	675.828	291.225	
Rocker pannel			**142.2437**		**123.241**		**84.83867**	**Average**
Lower hinge pillar			**396.241**		**364.164**		**298.328**	**Max**
Upper hinge pillar			**441.895**		**398.251**		**329.285**	**Max**

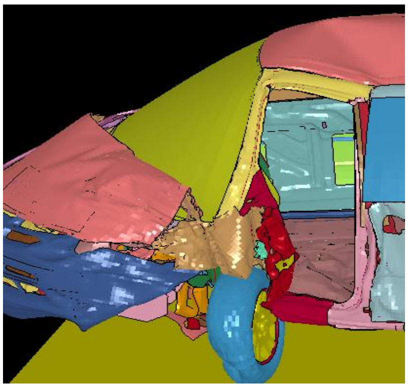

Figure 10. Vehicle deformation with Flat 50

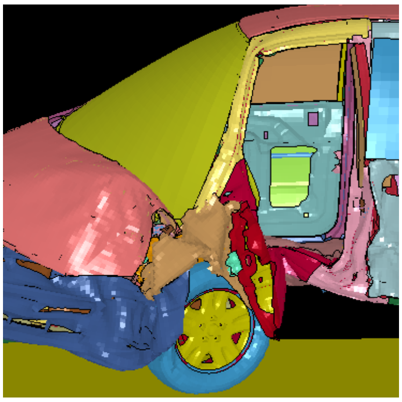

Figure 11. Vehicle deformation with Flat 150

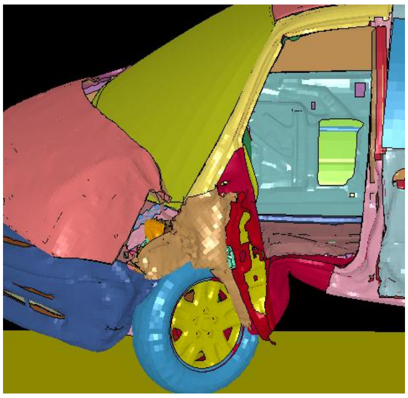

Figure 12. Vehicle deformation with Pole 250

4.2. Small-overlap rating

According to [3], the initial structural rating is based on comparing the measured intrusion with the rating guidelines, as shown in Figure 15. This rating may then be modified on the basis of additional observations about the structural integrity of the safety cage. Following [3, 15] the structure is rated based on sub-ratings for both the lower and upper occupant compartments. The measured intrusions in the lower and upper compartments falling in the "good" zone receive a structural sub-rating of "good" if no additional observations lead to a downgraded rating. Similarly, vehicles with all intrusion measures falling into one of the other three zones shown in Figure 15 receive sub-ratings of "acceptable", "marginal", or "poor". When intrusion measurements fall in different rating bands, the sub-rating generally reflects the band with the most measurements. However, the sub-rating is not more than one rating level better than the worst measurement.

For example, a vehicle with a poor measurement for the left instrument panel would not score better than marginal for the upper occupant compartment structure, even if all other upper occupant compartment scored as good. Where half the measurements are in one band and half are in another, the sub-rating is that of the worse band.

Intrusion measurements falling on a boundary value are considered to fall in the band that represents the better rating.

The overall structural rating takes the worse of the lower and upper occupant compartment sub-ratings if no additional observations lead to a downgraded rating. For example, a vehicle with a lower occupant compartment sub-rating of acceptable and upper occupant compartment sub-rating of marginal receives an overall structural rating of marginal.

Based on [3, 15], the results obtained in this study were rated as shown in Figure 15.

4.3. Load path

The vehicle deformation and load path in Figure 13 are based on the values in Table 2. Despite the differences in test configurations (crash partner, barrier geometry, barrier type) compare to [4], the load paths and deformation patterns showed differences depending on if the main longitudinal rail was missed (i.e., Flat 50 mode with 20% overlap) or not. If the main longitudinal rail was missed, the wheel was directly loaded and pushed rearward into the toepan/hinge pillar/-rocker panel, and the upper structures received additional loading. This loading pattern led to significant intrusion of both the lower and upper regions of the occupant compartment. When the main longitudinal rail was not missed, the upper hinge pillar received the most deformation, as shown in Figure 8.

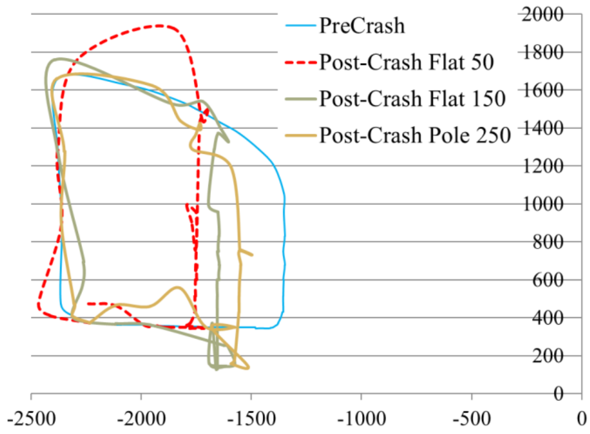

Figure 13. The vehicle deformation and load path

seen in real-world studies; occupant compartment intrusion has been identified as the primary injury mechanism in real-world crashes.

4.4. Optimal design vehicle structure model

The most commonly employed optimization process for a highly nonlinear problem with several design variables is to construct a multidimensional response surface as accurately as possible and seek an optimum solution on this surface. In this study, the design variables were chosen according to the design of experiments (DOE) method.

The algorithm was used to solve the following optimization problem:

Design objective: Minimum intrusion, $(R, L, U)_{min}$

Design factors: thicknesses of outer A-pillar (x1), A-pillar reinforcement (x2), inner A-pillar (x3), door frame (x4), rocker panel (x5), and lower hinge pillar (x6), as shown in Figure 14.

Design constraints: $X_{lower} < X < X_{upper}$

with $X = (x1, x2, x3, x4, x5, x6)^T$

where R, L, and U stand for the rocker panel, lower hinge pillar, and upper hinge pillar, respectively. X_{lower} and X_{upper} are the minimum and maximum values in the for the variable in the design range.

Table 3 lists the X_{lower} and X_{upper} for each component. The central composite was chosen for the design type. In this study, the high and low levels were set at the same time as when the experiments were performed.

Table 5 lists the objective values for all of the DOE samples; the best cases are highlighted. Those values were applied to the new model design. Figure 15 show the results of the new model crash test. Table 4 compares the intrusion in the occupant compartments with the original model.

The results in Table 4 demonstrate that the rating for the occupant compartment intrusion can be improved by strengthening the stiffness. In this study, the size optimization method was used to adjust the vehicle structure reinforcement by changing the thicknesses of the A-pillar, rocker panel, door frame, and lower hinge pillar. In this case, the thickness was changed by 20% (T 20). Table 3 lists the ranges of the design variables.

Table 4 lists the simulation results of the new design. When the same model was used for different modes, opposite results were obtained. Figure 15 compares the original model with the new model (T 20) in different modes. The improvements in the structure can be observed via the intrusion rating. In most cases, the deformation decreased with the changed thickness.

Table 3. Range of design variables (unit: mm)

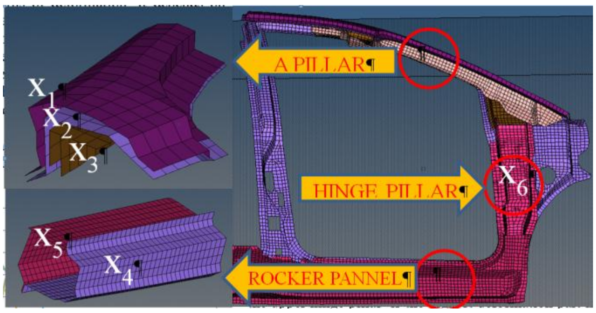

Figure 14. Illustration of design variables for vehicle structure

Table 5. Optimal values for variables using central composite design

Std Order	Run Order	Pt Type	Blk	A pillar outer	A pillar reinf	A pillar inner	Door frame	Rocker pannel	lower hinge pillar	Run	Blk	A	B	C	D	E	F
14	1	1	1	1.44	1.488	1.504	1.716	1.584	1.596	1	1	1.000	-1.000	-1.000	1.000	1.000	1.000
20	2	0	1	1.2	1.86	1.88	1.43	1.32	1.33	2	1	0.000	0.000	0.000	0.000	0.000	0.000
16	3	1	1	1.44	2.232	1.504	1.716	1.584	1.064	3	1	1.000	1.000	-1.000	1.000	1.000	-1.000
13	4	1	1	0.96	1.488	1.504	1.716	1.584	1.064	4	1	-1.000	-1.000	-1.000	1.000	1.000	-1.000
12	5	1	1	1.44	2.232	2.256	1.144	1.584	1.064	5	1	1.000	1.000	1.000	-1.000	1.000	-1.000
15	6	1	1	0.96	2.232	1.504	1.716	1.584	1.596	6	1	-1.000	1.000	-1.000	1.000	1.000	1.000
2	7	1	1	1.44	1.488	1.504	1.144	1.056	1.596	7	1	1.000	-1.000	-1.000	-1.000	-1.000	1.000
9	8	1	1	0.96	1.488	2.256	1.144	1.584	1.064	8	1	-1.000	-1.000	1.000	-1.000	1.000	-1.000
17	9	0	1	1.2	1.86	1.88	1.43	1.32	1.33	9	1	0.000	0.000	0.000	0.000	0.000	0.000
4	10	1	1	1.44	2.232	1.504	1.144	1.056	1.064	10	1	1.000	1.000	-1.000	-1.000	-1.000	-1.000
18	11	0	1	1.2	1.86	1.88	1.43	1.32	1.33	11	1	0.000	0.000	0.000	0.000	0.000	0.000
8	12	1	1	1.44	2.232	2.256	1.716	1.056	1.064	12	1	1.000	1.000	1.000	1.000	-1.000	-1.000
3	13	1	1	0.96	2.232	1.504	1.144	1.056	1.596	13	1	-1.000	1.000	-1.000	-1.000	-1.000	1.000
11	14	1	1	0.96	2.232	2.256	1.144	1.584	1.596	14	1	-1.000	1.000	1.000	-1.000	1.000	1.000
1	15	1	1	0.96	1.488	1.504	1.144	1.056	1.064	15	1	-1.000	-1.000	-1.000	-1.000	-1.000	-1.000
10	16	1	1	1.44	1.488	2.256	1.144	1.584	1.596	16	1	1.000	-1.000	1.000	-1.000	1.000	1.000
5	17	1	1	0.96	1.488	2.256	1.716	1.056	1.064	17	1	-1.000	-1.000	1.000	1.000	-1.000	-1.000
6	18	1	1	1.44	1.488	2.256	1.716	1.056	1.596	18	1	1.000	-1.000	1.000	1.000	-1.000	1.000
7	19	1	1	0.96	2.232	2.256	1.716	1.056	1.596	19	1	-1.000	1.000	1.000	1.000	-1.000	1.000
19	20	0	1	1.2	1.86	1.88	1.43	1.32	1.33	20	1	0.000	0.000	0.000	0.000	0.000	0.000
40	21	0	2	1.2	1.86	1.88	1.43	1.32	1.33	21	2	0.000	0.000	0.000	0.000	0.000	0.000
33	22	1	2	0.96	1.488	2.256	1.716	1.584	1.596	22	2	-1.000	-1.000	1.000	1.000	1.000	1.000
21	23	1	2	0.96	1.488	2.256	1.144	1.056	1.596	23	2	-1.000	-1.000	1.000	-1.000	-1.000	1.000
34	24	1	2	1.44	1.488	2.256	1.716	1.584	1.064	24	2	1.000	-1.000	1.000	1.000	1.000	-1.000
23	25	1	2	0.96	2.232	2.256	1.144	1.056	1.064	25	2	-1.000	1.000	1.000	-1.000	-1.000	-1.000
26	26	1	2	1.44	1.488	1.504	1.716	1.056	1.064	26	2	1.000	-1.000	-1.000	1.000	-1.000	-1.000
24	27	1	2	1.44	2.232	2.256	1.144	1.056	1.596	27	2	1.000	1.000	1.000	-1.000	-1.000	1.000
37	28	0	2	1.2	1.86	1.88	1.43	1.32	1.33	28	2	0.000	0.000	0.000	0.000	0.000	0.000
30	29	1	2	1.44	1.488	1.504	1.144	1.584	1.064	29	2	1.000	-1.000	-1.000	-1.000	1.000	-1.000
29	30	1	2	0.96	1.488	1.504	1.144	1.584	1.596	30	2	-1.000	-1.000	-1.000	-1.000	1.000	1.000
31	31	1	2	0.96	2.232	1.504	1.144	1.584	1.064	31	2	-1.000	1.000	-1.000	-1.000	1.000	-1.000
39	32	0	2	1.2	1.86	1.88	1.43	1.32	1.33	32	2	0.000	0.000	0.000	0.000	0.000	0.000
22	33	1	2	1.44	1.488	2.256	1.144	1.056	1.064	33	2	1.000	-1.000	1.000	-1.000	-1.000	-1.000
28	34	1	2	1.44	2.232	1.504	1.716	1.056	1.596	34	2	1.000	1.000	-1.000	1.000	-1.000	1.000
35	35	1	2	0.96	2.232	2.256	1.716	1.584	1.064	35	2	-1.000	1.000	1.000	1.000	1.000	-1.000
36	36	1	2	1.44	2.232	2.256	1.716	1.584	1.596	36	2	1.000	1.000	1.000	1.000	1.000	1.000
25	37	1	2	0.96	1.488	1.504	1.716	1.056	1.596	37	2	-1.000	-1.000	-1.000	1.000	-1.000	1.000
32	38	1	2	1.44	2.232	1.504	1.144	1.584	1.596	38	2	1.000	1.000	-1.000	-1.000	1.000	1.000
27	39	1	2	0.96	2.232	1.504	1.716	1.056	1.064	39	2	-1.000	1.000	-1.000	1.000	-1.000	-1.000
38	40	0	2	1.2	1.86	1.88	1.43	1.32	1.33	40	2	0.000	0.000	0.000	0.000	0.000	0.000
44	41	-1	3	1.2	2.7402	1.88	1.43	1.32	1.33	41	3	0.000	2.366	0.000	0.000	0.000	0.000
52	42	-1	3	1.2	1.86	1.88	1.43	1.32	1.959	42	3	0.000	0.000	0.000	0.000	0.000	2.366
48	43	-1	3	1.2	1.86	1.88	2.1067	1.32	1.33	43	3	0.000	0.000	0.000	2.366	0.000	0.000
53	44	0	3	1.2	1.86	1.88	1.43	1.32	1.33	44	3	0.000	0.000	0.000	0.000	0.000	0.000
43	45	-1	3	1.2	0.9798	1.88	1.43	1.32	1.33	45	3	0.000	-2.366	0.000	0.000	0.000	0.000
49	46	-1	3	1.2	1.86	1.88	1.43	0.6954	1.33	46	3	0.000	0.000	0.000	0.000	-2.366	0.000
50	47	-1	3	1.2	1.86	1.88	1.43	1.9446	1.33	47	3	0.000	0.000	0.000	0.000	2.366	0.000
46	48	-1	3	1.2	1.86	2.77	1.43	1.32	1.33	48	3	0.000	0.000	2.366	0.000	0.000	0.000
51	49	-1	3	1.2	1.86	1.88	1.43	1.32	0.701	49	3	0.000	0.000	0.000	0.000	0.000	-2.366
45	50	-1	3	1.2	1.86	0.99	1.43	1.32	1.33	50	3	0.000	0.000	-2.366	0.000	0.000	0.000
42	51	-1	3	1.768	1.86	1.88	1.43	1.32	1.33	51	3	2.366	0.000	0.000	0.000	0.000	0.000
54	52	0	3	1.2	1.86	1.88	1.43	1.32	1.33	52	3	0.000	0.000	0.000	0.000	0.000	0.000
47	53	-1	3	1.2	1.86	1.88	0.7533	1.32	1.33	53	3	0.000	0.000	0.000	-2.366	0.000	0.000
41	54	-1	3	0.632	1.86	1.88	1.43	1.32	1.33	54	3	-2.366	0.000	0.000	0.000	0.000	0.000

Table 4. Intrusion of occupant compartments in three modes for different thicknesses (unit: mm)

Node to node	Components	Flat 50 Intrusion T 20	Flat50 Original Intrusion	Flat 150 Intrusion T 20	Flat 150 Original Intrusion	Pole 250 Intrusion T 20	Pole 250 Original Intrusion	Note
2090591-2096390	Rocker pannel 1	53.115	85.348	39.537	101.887	11.234	78.253	
2090591-2095742	Rocker pannel 2	120.032	140.942	89.145	101.735	25.775	84.444	
2090591-2100681	Rocker pannel 3	169.191	200.441	139.217	166.1	80.77	91.819	
2090591-2060508	Lower hinge pillar 1	303.753	393.922	221.292	315.378	96.971	298.328	
2090591-2060483	Lower hinge pillar 2	283.174	396.241	230.57	364.164	137.636	249.224	
2090591-2100727	Lower hinge pillar 3	297.527	375.768	226.251	357.737	148.461	260.762	
2090591-2084338	Upper hinge pillar 1	297.89	348.84	170.54	398.251	118.779	329.285	
2090591-2084327	Upper hinge pillar 2	281.044	441.895	175.89	382.696	93.094	240.641	
2090591-2084128	Upper hinge pillar 3	250.336	308.384	160.879	273.101	128.79	291.225	
	Rocker pannel	**114.1127**	**142.244**	**89.29967**	**123.241**	**39.2597**	**84.8387**	**Average**
	Lower hinge pillar	**303.753**	**396.241**	**230.57**	**364.164**	**148.461**	**298.328**	**Max**
	Upper hinge pillar	**297.89**	**441.895**	**175.89**	**398.251**	**128.79**	**329.285**	**Max**

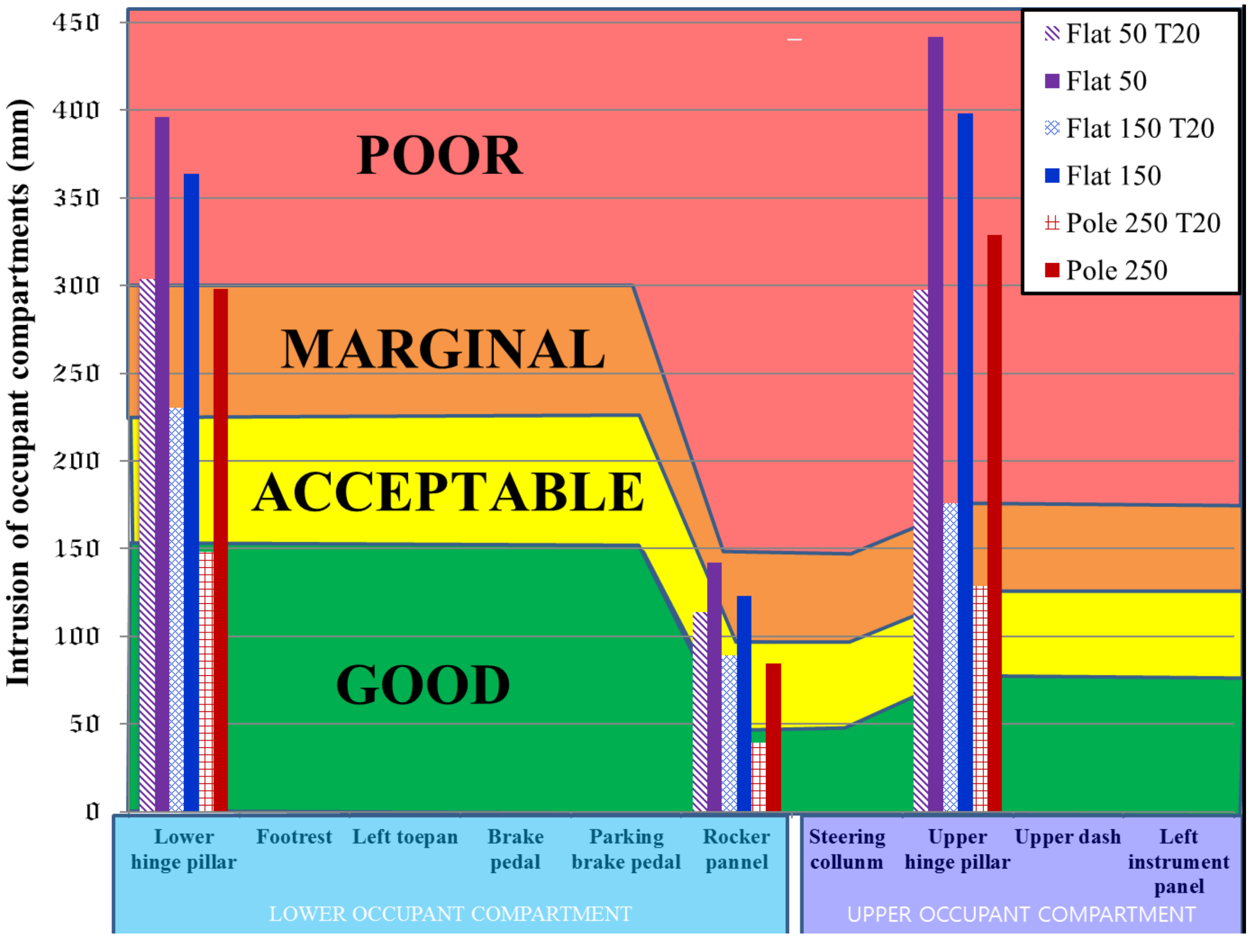

Figure 15. Guidelines for rating occupant compartment intrusion with different modes

5. CONCLUSION

In this study, a minivan FE model was used to analyze the vehicle body in the event of a small-overlap frontal crash with three types of barriers. The simulation results of the original and new design model were analyzed in three modes: Flat 50, Flat 150, and Pole 250.

The Flat 50 mode displayed the most serious intrusion; the rocker panel and lower hinge pillar showed the most deformation. In addition, the A-pillar was bent and moved upward. The left wheel was turned 90° with severe damage. The overall structural evaluation for this mode was “poor.”

The Flat 150 mode showed the second most serious intrusion; the rocker panel was bent, and the A-pillar moved backward. In this mode, the overall structural rating was upgraded to “marginal.”

The Pole 250 mode showed the least serious intrusion; the rocker panel became bent, the A-pillar moved backward, and the vehicle model sliced out of the barrier. In this mode, the overall structural rating was upgraded to “acceptable.”

The poor results indicate that most vehicles are just not designed for small-overlap impacts with rigid barriers. Traditional crash absorption structures are completely bypassed during the event, which exposes the vehicle safety structure to greater deformation and the occupant to stronger deceleration.

At present, most vehicles are designed to use the entire front end to absorb an impact, and crash testing has focused on only the driver’s side. This is why almost all cars currently available commercially are rated as “poor” or “marginal” by the IIHS.

Future extensions of this research could include improving the front side member via various barriers in the event of a SOFI. The limitations of the thickness optimization method do not satisfy the requirements for the three barrier types with small overlap. Based on the drawbacks of this method, future work will involve improving the vehicle structure for SOFI tests with various barriers by optimizing the cross-section design of multiple components such as the A-pillar, rocker panel, and longitudinal rail. A new active frame rail will be proposed to engage the barriers and other reinforcements in the key cross members.

ACKNOWLEDGMENT

This work was supported in part by the research program 2015 of Kookmin University in korea.

REFERENCES

[1] Sherwood, C. Insurance institute for highway safety (2012). *An update on the IIHS small-overlap research program*, 1-35.

[2] Insurance institute for highway safety (2012). Front small-overlap crashworthiness evaluation crash test protocol (version I, II), 1-25.

[3] Insurance institute for highway safety (2012). S*mall-overlap program protocol and rating guidelines*. 1-17.

[4] Sherwood, C., Mueller, B., Nolan, J. m., Zuby, D. S. and Lund, A. K. (2013). IIHS. Development of a frontal small-overlap crashworthiness evaluation test. *Traffic injury prevention*. DOI:10.1080/15389588. 790539.

[5] Kikuchi,T., Naokao, T., Watanabe, T., Saeki, H. and Okabe, T. (2012). An investigation of injury factors concerning drivers in vehilces involved in small-overlap fronta; crashes. *SAE paper*, NO 2012-01-0599.

[6] Bois, P.D., Chou, C.C., Fileta, B.B., Khalil, T.B., King, A.L., Mahmood, H.F., Mertz, H.J., Wismans, J. (2004). *Vehicle crashworthiness and occupant protection*. 11-176. Michigan.

[7] Brumbelow, M.L., Zuby, D.S. (2012). Impact and injury patterns in frontal crashes of vehicles with good ratings for frontal crash protection. *IIHS paper* No 09-0257. USA.

[8] Nolan, J. IIHS. (2012). *Results of small-overlap frontal crash tests*.1-18. Germany.

[9] Hong, S.W., Park, C.K., Mohan, P. (2008). A study of the IIHS frontal pole impact test. *SAE paper*, NO 2008-01-0507.

[10] Park, B. T., Partyka, S. C., Morgan, R. M., Hackney, J. R., Lee, J. and Summers, L. (2000). Comparison of vehicle structural intergrity and occupant injury potential in full-frontal and offset-frontal crash tests. *SAE paper*, NO 2000-01-0879.

[11] Chen, G., Shi , M. F. and Tyan, T. (2012). Optimized AHSS structures for vehicle side impact. *SAE paper*, NO 2012-01-0044.

[12] Halloway, D. E., Pintar, F., Saunders, J. and Anelli, A. B. (2012). Classifiers to augment the CDC system to distinguish the role of structure in a frontal impact taxonomy. *SAE paper*, NO 2012-01-0575.

[13] Jakobsson, L., Mcinally, G., Axelson, A., Lindman, M., Kling, A., Broberg, T., Fermer, M. and Wagstrom, L. (2013). Severe frontal collisions with partial overlap-two decades of car safety development. *SAE paper*, NO 2013-01-0759.

[14] Chittepu, K. (2011). Significance of robustness evaluation in crash analysis. *SAE paper*, NO 2011-26-0017.

[15] Sherwood, C. (2013). Insurance institute for highway safety (IIHS). *An update on the IIHS small-overlap ratings program*. 1-13. USA.

[16] National Crash Analysis Center (NCAC) The George Washington University. (2005). *FE Model of Dodge Grand Caravan*, 1-13.

[17] Hallquist, J.O. (2007). *LS-DYNA Keyword User Manual*, Livermore Software Technology Corporation.

[18] Murri, R., Caviezel, S., Gerster, B. (2013). Relevance of the IIHS small-overlap crash test in Europe. *Internal study DTC Dynamic Test Center AG*, Report number pSi-13-0130.

[19] http://www.iihs.org

[20] http://www.highwaysafe.org

[21] http://www.ncac.gwu.edu/vml/models.html